Materials Science-Poland, *Vol. 27*, *No. 4/1*, *2009*

High temperature impedance spectroscopy study of non-stoichiometric bismuth zinc niobate pyrochlore

K. B. TAN[1*], C. C. KHAW[2], C. K. LEE[3], Z. ZAINAL[1], Y. P. TAN[1], H. SHAARI[1]

[1]Faculty of Science, Universiti Putra Malaysia, 43400 Serdang, Selangor, Malaysia

[2]Faculty of Engineering and Science, Universiti Tunku Abdul Rahman, 53300 Kuala Lumpur, Malaysia

[3]Academic Science Malaysia, 902-4 Jalan Tun Ismail, 50480 Kuala Lumpur, Malaysia

Single phase non-stoichiometric bismuth zinc niobate, $Bi_3Zn_{1.84}Nb_3O_{13.84}$ was prepared by a conventional solid state method. The sample was refined and fully indexed on the cubic system, space group *Fd*3*m*, $Z = 4$ with $a = 10.5579(4)$ Å. Electrical characterisation was performed using an ac impedance analyser over the temperature range of 25–850 °C and frequency range of 5 Hz–3 MHz. Typical dielectric response was observed in $Bi_3Zn_{1.84}Nb_3O_{13.84}$ with high relative permittivity, low dielectric loss and negative temperature coefficient of capacitance, with the values of 147, 0.002 and –396 ppm/°C, at 100 kHz at ambient temperature, respectively. The material is highly resistive, with the conductivity of 10^{-21} $ohm^{-1}\cdot cm^{-1}$ and a high activation energy of ~1.59 eV.

Key words: *activation energy; bismuth zinc niobate; dielectric response; impedance spectroscopy; pyrochlore*

1. Introduction

Due to its excellent properties, advanced ceramics have been used in a wide range of industrial applications such as electrical and electronic components, superconductors, catalyst and automobile components [1–3]. The study of advanced ceramic materials involves many disciplines, including chemistry, physics, mechanical engineering, materials science and metallurgy. Both electroceramics and structural ceramics are classified as advanced ceramics, and they have different applications. Applications of electroceramics involve electrical and magnetic properties, whereas applications of structural ceramics mainly rely on their mechanical behaviour [4].

One of the promising candidates in electroceramics is bismuth pyrochlore [5]. Pure bismuth oxides are highly reactive, volatile and thermally unstable with poly-

*Corresponding author, e-mail: tankb@science.upm.edu.my

morphic transitions in which monoclinic α-Bi_2O_3 transforms to a defect fluorite δ-Bi_2O_3 above 729 °C, and then followed by the formation of two metastable phases, tetragonal β-Bi_2O_3 and body-centred cubic γ-Bi_2O_3, while cooling down [6]. However, bismuth derivatives are suitable and cost effective for various commercial applications, particularly in microwave and radio frequency applications, due to their low firing temperatures This follows the trend of miniaturisation with passive integration using multilayer ceramic technology whereby active or passive components are laminated and co-fired at low temperatures. In general, pyrochlore materials have the formula $A_2B_2O_7$, indicating the existence of two different crystallographic sites, namely a relatively larger 8- coordinate A site and a smaller 6-coordinate B site within the structure. These sites are commonly occupied by a combination of A^{3+} and B^{4+} cations, A^{2+} and B^{5+} cations or other combinations with a required average mixed valency [7]. By far the most extensively studied Bi-based dielectrics are the cubic pyrochlore $Bi_{3/2}ZnNb_{3/2}O_7$ ($k' = 150$, $t_k = -400$ ppm/°C) and the monoclinic zirconolite phase ($k' = 80$, $t_k = 200$ ppm/°C). Their permittivities have temperature dependencies of opposite signs. Consequently, the two dielectrics are considered to be a good pair to obtain new dielectrics with good temperature dependences by combining them.

An "ideal" composition for a pyrochlore phase in the Bi_2O_3–ZnO–Nb_2O_5 (BZN) system could be $Bi_3Zn_2Nb_3O_{14}$, referred to as P, in which the expectation is that a part of Zn and all Bi would be disordered over the large, 8-coordinate A sites; the remainder of Zn, together with Nb, would be disordered over the octahedral B-sites. However, it has been shown that the material of composition $Bi_3Zn_2Nb_3O_{14}$ contains excessive ZnO as a second phase and lies outside the BZN subsolidus solid solution area [9–13]. The pure phase composition was confirmed to be ZnO deficient by electron probe microanalysis and a combination study of electron, neutron and X-ray diffraction.

Since the 1990's many of the fundamental aspects of BZN materials have been clarified. However, there are inconsistencies in the literature regarding the characterisation of BZN materials, particularly electric permittivities of multiphase samples from various researchers are scattered in the range of 80–120 [9–13]. Preliminary electrical studies on Bi_2O_3–ZnO–Nb_2O_5 ternary system indicate that these materials are highly insulating and their conductivities are not likely to be determined at temperatures below 500 °C. However, it is possible to measure permittivities at high frequencies at ambient temperatures and above. An overall objective of electrical characterisation is to investigate the effects of composition and temperature on the bulk permittivity, i.e. variation of bulk permittivity with composition and whether the permittivity varies, positively or negatively with temperature. Investigation of various possible sources of error and variations in permittivity measurements are therefore indispensable before a firm conclusion can be drawn in correlating permittivity with density, sintering temperature and electrodes. The electrical data were collected on samples whose sintering conditions have been optimised with respect to the capacitance value, bismuth loss and pellet density. The focus of this paper is on the high

temperature electrical behaviour of optimised $Bi_3Zn_{1.84}Nb_3O_{13.84}$ via a systematic impedance spectroscopy study.

2. Experimental

Cubic pyrochlore $Bi_3Zn_{1.84}Nb_3O_{13.84}$ was prepared via conventional solid state reactions using Bi_2O_3 (Alfa Aesar, 99.99 %), ZnO (Alfa Aesar, 99.99 %), and Nb_2O_5 (Alfa Aesar, 99.99 %) as starting materials. ZnO and Nb_2O_5 were dried at 600 °C while Bi_2O_3 was dried at 300 °C for 3 h prior to weighing. Stoichiometric quantities of the oxides were weighted and mixed with sufficient volume of acetone in an agate mortar to ensure the homogeneity of the mixture. The resulting powder was transferred into a gold boat and pre-fired at 700 °C for 24 h (below Bi_2O_3 melting point of ca. 825 °C) in a Carbolite muffle furnace. Subsequently, the mixture was fired at temperatures of 800 °C and 950 °C for 24 h with intermediate regrinding. The phase purity of the sample was examined at room temperature by X-ray diffraction using a Shimadzu X-ray powder diffractometer XRD-6000 equipped with a diffracted-beam graphite monochromator, with CuK_α radiation (1.5418×10^{-10} m). Pellets of a single phase sample were prepared using a stainless steel die measuring 8 mm in diameter. A sufficient amount of powder was added, cold pressed uniaxially, and sintered at 1050 °C in order to increase the mechanical strength and to reduce the intergranular resistance in the pellets. Gold paste (Engelhard) was smeared and hardened onto parallel faces of the ceramics. The pellets with gold electrodes attached were placed on a conductivity jig and inserted in a horizontal tube furnace. The pellets were characterised using an ac Hewlett Packard LF HP4192A impedance analyser over the frequency range from 5 Hz to 1.3×10^7 Hz with the applied voltage of 100 mV. Conductivity measurements were carried out over the temperature range of 28–850 °C on heating and cooling cycles at each 50 °C interval. The samples were allowed to equilibrate at each temperature for 30 min prior to measurement. Most measurements were made in air, and, if necessary, in oxygen free nitrogen (OFN) at the flow rate of 80 cm^3/min for reducing atmosphere study. The nitrogen gas was supplied to the sealed tube furnace for 1 h in order to create an equilibrated nitrogen atmosphere prior to measurement.

3. Results and discussion

The electrical properties of optimised $Bi_3Zn_{1.84}Nb_3O_{13.84}$ pellets with the density of ca. 90 % sintered at 1050 °C were determined by ac impedance spectroscopy over the frequency range of 5 Hz–13 MHz in air. The measured impedance data are represented in the Nyquist form with a typical complex plane plot (Z'' vs. Z'). The impedance is normalised by the geometric factor and represented in the form of the dependence $\rho^* = Z^*(S/d) = \rho' + j\rho''$ where ρ^* is the complex resistivity and S/d is the geometric factor. The parameters S and d represent the area and the separation of the electrodes

[14, 15]. Perfect semicircles are only observed in the Cole–Cole plots of cubic pyrochlore $Bi_3Zn_{1.84}Nb_3O_{13.84}$ above 550 °C (Fig. 1).

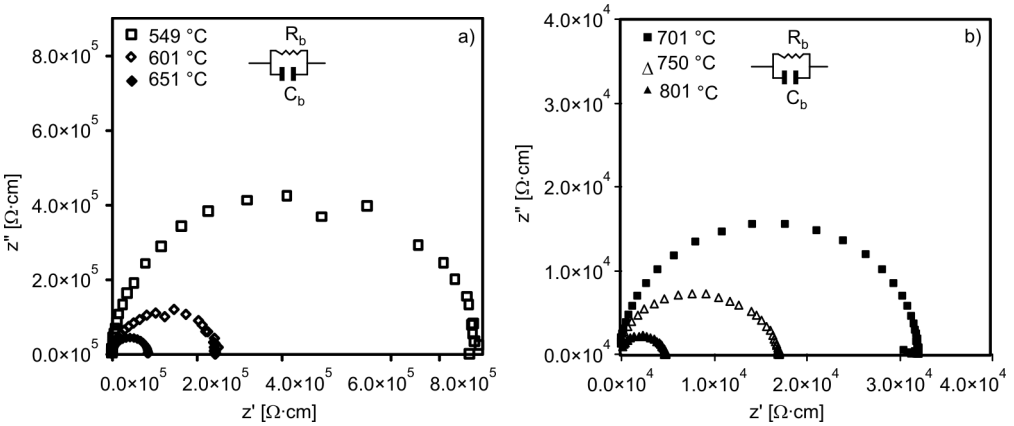

Fig. 1. Cole–Cole plots of $Bi_3Zn_{1.84}Nb_3O_{13.84}$ at various temperatures

The impedance data can be represented by the equivalent circuit shown in the inset of Fig. 1. The circuit consists of parallel R and C elements of the bulk material and the total impedance Z^* for the circuit is given by:

$$Z^* = \frac{1}{j\omega C + \frac{1}{R}} = \frac{R}{1 + j\omega CR} = Z' - jZ'' \tag{1}$$

An associated capacitance of 1.19×10^{-11} F·cm^{-1} (after correction for jig) is obtained at 549 °C and this corresponds to the bulk properties of the material. The corresponding bulk resistivities, R_b from ca. 8.3×10^5 to ca. 2×10^3 Ω·cm over the temperature range 550–850 °C are obtained from the intercept on the real part of the impedance. This could be associated with the increase in thermally activated drift mobility of electric charge carriers according to the hopping conduction mechanism. In addition, the resistivity falls as the temperature increases, because the probability of carriers being promoted into the conduction band, or being transferred from one defect to another is governed by thermal fluctuations which are described by the Boltzmann statistics [16]. On the other hand, higher dielectric polarisation may result in higher electric permittivities and higher losses as the temperature increases [17].

For a highly resistive material, the Nyquist diagram is not completely defined as the data fitting may lead to a gross error. Hence, the capacitance and permittivity value can be extracted based on the electrical response in a high frequency range of 10^5–10^7 Hz using the equation $-Z'' = 1/(jC_b 2\pi f)$ where Z'' is the imaginary part of impedance, j is the operator $(-1)^{1/2}$ and ω is the angular frequency. The capacitance C_b of the bulk material can be determined from the slope of the plot $-Z''$ vs. $1/2\pi f$. A bulk capacitance of 1.19×10^{-11} F·cm^{-1} (after correction for the stray capacitance from the empty

jig) is obtained for $Bi_3Zn_{1.84}Nb_3O_{13.84}$ at 549 °C (Fig. 2) which agrees reasonably well with that obtained from the Cole–Cole plot ($\omega RC_b = 1$).

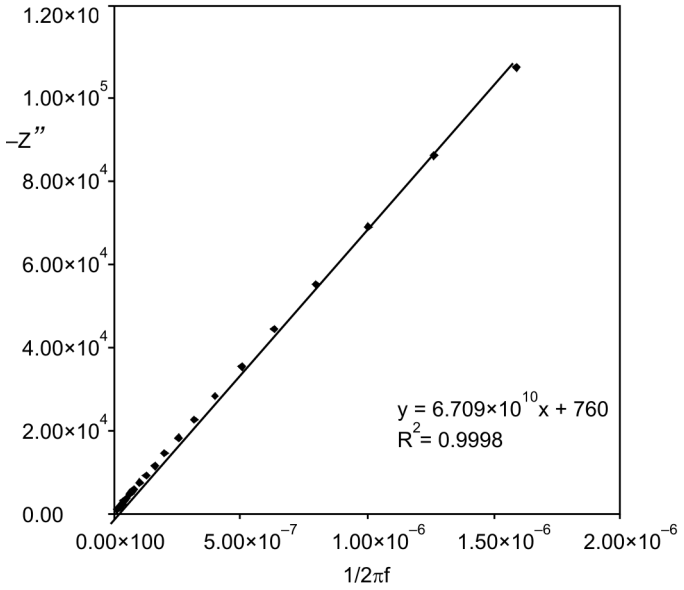

Fig. 2. Imaginary part of impedance, Z'', in function of the reciprocal angular frequency, at 549 °C

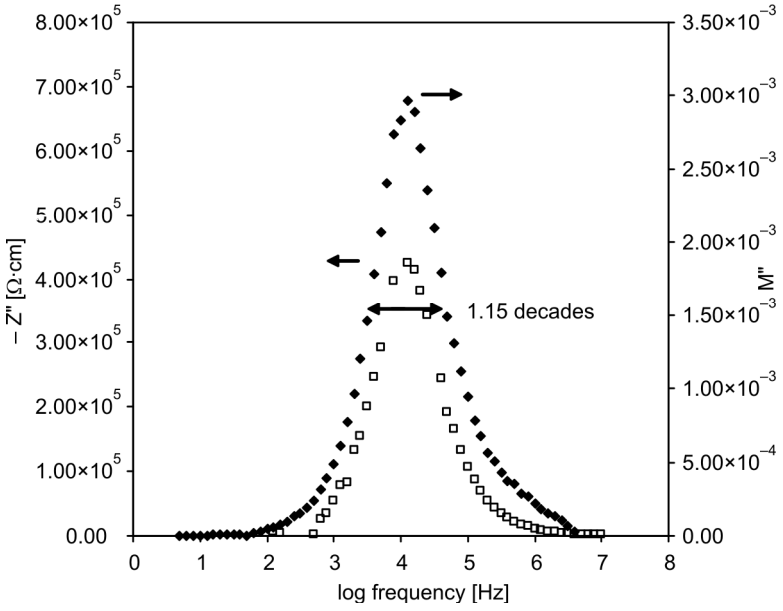

Fig. 3. Combined Z'' and M'' spectroscopic plots for cubic pyrochlore $Bi_3Zn_{1.84}Nb_3O_{13.84}$ at 549 °C

The impedance data of the material are further examined using the combined spectroscopic plots of imaginary components of the complex impedance, Z'' and electric modulus, M''. The frequency maxima of Z'' and M'' should be coincident, and the full width at a half maximum (FWHM) should be equal to 1.14 decade for an ideal Debye response representing bulk properties. There appears to be no grain boundary effect as two overlapping peaks with the FWHM value of ca. 1.15 decades are obtained (Fig. 3), indicating that the material is homogeneous.

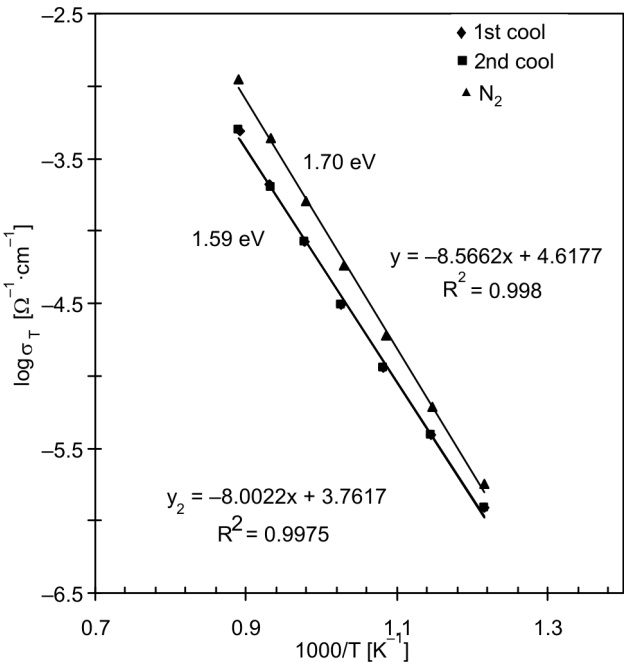

Fig. 4. Conductivity Arrhenius plots of cubic pyrochlore, $Bi_3Zn_{1.84}Nb_3O_{13.84}$

Figure 4 shows the electrical conductivity of the material in function of temperature. The Arrhenius law is applied in order to correlate the observed behaviour with a general dependence, $\sigma = \sigma_0 \exp(-E_a/kT)$ where σ_0 represents the pre-exponential factor, E_a is the apparent activation energy of the conduction process, k is Boltzmann's constant and T is absolute temperature. The conductivity data are reproducible and reversible in heat–cool cycles with a high activation energy of of 1.59 eV. Usually, high activation energy is required for the occurrence of a hopping type electronic mechanism, especially with the presence of defects of the oxygen vacancy in the pyrochlore structure [14, 15]. The conductivity at room temperature is determined by the data extrapolation. Cubic pyrochlore, $Bi_3Zn_{1.84}Nb_3O_{13.84}$, exhibits the conductivity of an order lower than that of bismuth zinc antimonite (BZS) with the value of $10^{-21}\ \Omega^{-1}\cdot cm^{-1}$ at room temperature. The high resistivity of Bi based pyrochlores has been noted in literature and these materials are mainly used for dielectric applications [18].

Oxides are susceptible to oxygen loss with creation of anion vacancies and associated reduction at high temperatures, especially under reducing atmosphere where a process, $2O^{2-} \rightarrow O_2 + 4e^-$ takes place. In a nitrogen atmosphere, $Bi_3Zn_{1.84}Nb_3O_{13.84}$ exhibits n-type conduction with higher conductivity and the activation energy of 1.70 eV (Fig. 4). This may be considered as evidence that cation disordered pyrochlores (A ↔ B exchange) exhibit a high level of intrinsic oxygen Frenkel disorder (48*f* → 8*b*). It was suggested by Clayton et al. [19] that $Bi_3Zn_2Nb_3O_{14}$ pyrochlore disclosed a n- to p-type behaviour in function of temperature and partial pressure of oxygen. The p-type conductivity dominated at high pO_2, under oxidizing conditions and n-type conductivity dominated at low pO_2 with considerable ionic contribution to the conductivity, due to the presence of the shallow minimum in conductivity measurements.

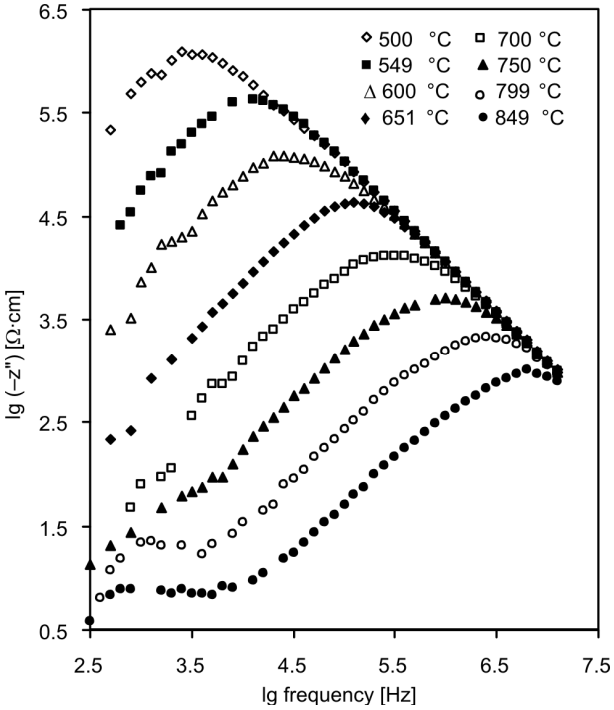

Fig. 5. Imaginary part of impedance in function of frequency for cubic pyrochlore, $Bi_3Zn_{1.84}Nb_3O_{13.84}$ at various temperatures

A dispersion of imaginary impedance, Z'' in function of frequency is shown in Fig. 5. The maxima of the curves shift towards a higher frequency region as the measuring temperature increases; this indicates the presence of a polarisation process in the dielectric material. Peak frequencies in Fig. 5 are used in an Arrhenius plot (peak frequency type) to show its dependence on temperature. Figure 6 shows the evolution of the peak frequency that follows the Arrhenius law with an apparent activation energy

of 1.55 eV. This value is in good agreement with the activation energy, previously calculated from the conductivity Arrhenius plot, i.e. 1.59 eV. This suggests strongly that the electrical behaviour of cubic pyrochlore $Bi_3Zn_{1.84}Nb_3O_{13.84}$ is influenced by the polarisation phenomenon in the crystalline lattice and that the conduction mechanism is of the hopping type [14, 15].

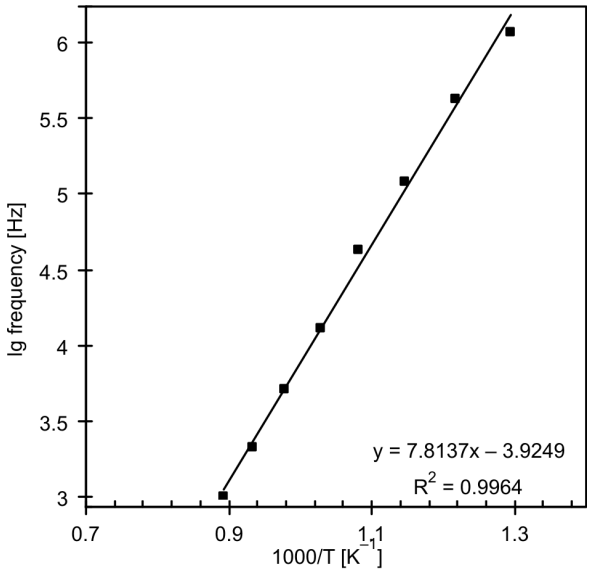

Fig. 6. Arrhenius plot for the peak frequency, lg(–Z'') of cubic pyrochlore, $Bi_3Zn_{1.84}Nb_3O_{13.84}$

The electric modulus is inversely proportional to the capacitance C. The peak heights of the modulus plots (Fig. 7) are independent of temperature, indicating that $Bi_3Zn_{1.84}Nb_3O_{13.84}$ does not exhibit ferroelectric properties in the temperature range under study. Similarly, the dielectric relaxation behaviour of ideal BZN cubic pyrochlore, $Bi_3Zn_2Nb_3O_{14}$, has been studied and it was suggested to be neither a dipolar glass nor a relaxor ferroelectric [20]. The complex dielectric response of $Bi_3Zn_2Nb_3O_{14}$ between 100 Hz and 100 kHz revealed a dielectric relaxation below the polar phonon frequencies. Relaxation at room temperature was observed at the frequency of 10^8 Hz, and the high frequency limit of relaxation frequencies was nearly temperature independent. The relaxation was postulated to be associated with hopping of disordered Bi and Zn atoms at A sites (each of the A atoms occupy one of 6 equivalent, closely spaced positions) and hopping of O′ atoms among 12 sites [20].

The complex electric permittivity ε^* can be expressed as a complex number

$$\varepsilon^* = \varepsilon'(\omega) - j\varepsilon''(\omega) \tag{2}$$

where ε′ and ε″ are the real and imaginary parts of the complex permittivity. Figure 8 illustrates the relative permittivity of $Bi_3Zn_{1.84}Nb_3O_{13.84}$ in function of frequency. High

dispersion characteristics in the curves at frequencies lower than 1 kHz could be attributed to the dielectric material behaviour where the conduction mechanism of a hopping type is present [14, 15]. This is probably due to atomic defects in cubic pyrochlores where intrinsic oxygen vacancies are present.

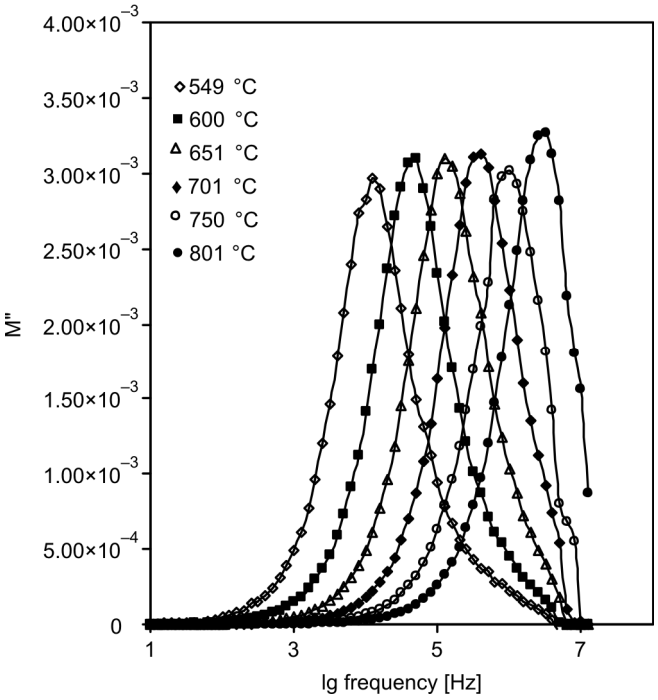

Fig. 7. Imaginary part of the electrical modulus in function of frequency

On the other hand, permittivity depends on the concentration of defects and the extent to which the internal field is raised above the applied field. Occurrence of a continuous flow of current rather than a limited oscillation between sites is noted to be due to high concentration of defects and/or high probability of hopping events. This contribution to the permittivity is small while the resistivity remains at a sufficiently high level for the dielectric of practical interest [16]. The degree of dispersion decreases as the frequency increases. In the frequency range of $10–10^3$ kHz, a frequency-independent response is observed over the entire temperature range studied (Fig. 8). This may be attributed to the inherent characteristic of dielectric materials as the oscillating system cannot follow the resonant frequency or jumping frequency ω_r in an applied field.

Figure 9 illustrates the real part of complex permittivity in function of temperature at several frequencies. The decline in permittivity in the temperature range of 25–400 °C (100–1000 kHz) indicates a negative temperature coefficient of permittivity of ca. 396 ppm/°C which is comparable to the reported value –400 ppm/°C [21, 22].

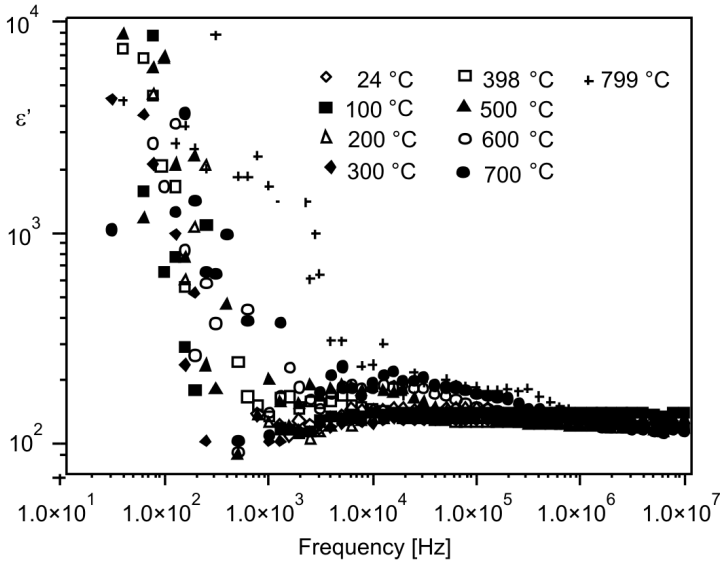

Fig. 8. Permittivity, ε′ in function of frequency at various temperatures

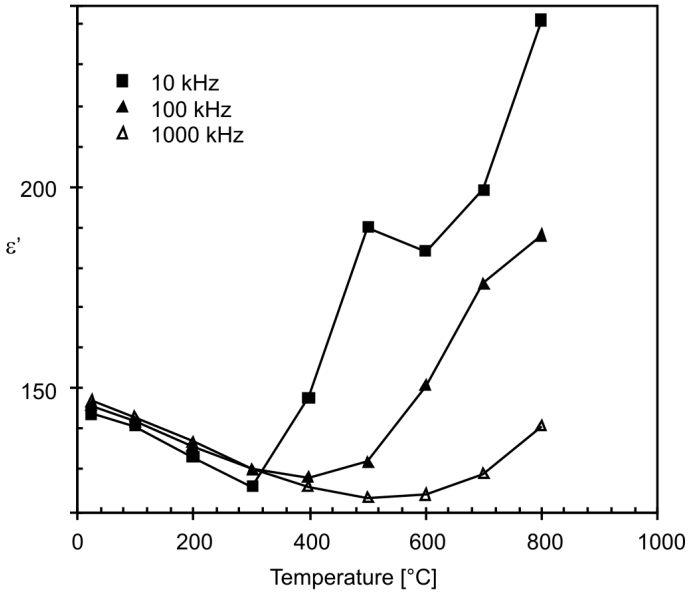

Fig. 9. Real part of complex permittivity in function of temperature at several frequencies

The dielectric loss can be expressed as

$$\tan\delta = \frac{\varepsilon''(\omega)}{\varepsilon'(\omega)} \tag{3}$$

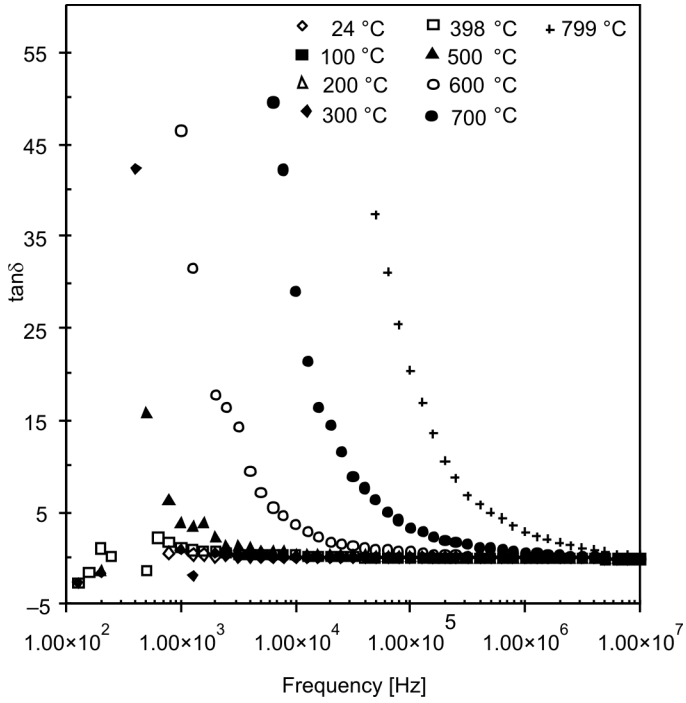

Fig. 10. Dielectric losses, tanδ, in function of frequency at several temperatures

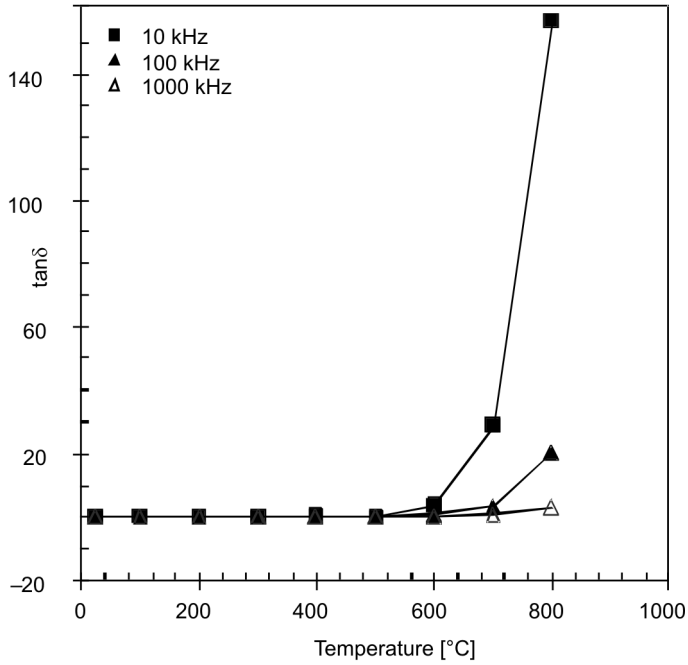

Fig. 11. Dielectric losses, tanδ, in function of temperature at several frequencies

A dense and pore free structure is a prerequisite for a low loss dielectric, as the pores may take up moisture which results in a higher dielectric loss, particularly if soluble ions are leached from the solid phase. The dielectric losses at various temperatures are shown in Fig. 10. All curves display a similar frequency independent behaviour below 500 °C. Above 500 °C, an appreciable increase in the dielectric losses is observed. Dielectric losses are strongly dependent on frequencies, i.e. lower loss is observed at higher frequencies (Fig. 11). The behaviour below 500 °C could be associated with the non-frequency dependence of dielectric loss (above kilohertz region) of BZN cubic pyrochlore with hopping conduction mechanism mentioned earlier. High dielectric loss at low frequencies is possibly due to time availability for the displacement of defects. Energy is lost through the movement of the screening charge (adjustment of surrounding ions relative to their state when the defect is absent) against the applied field. The ratio of energy lost, W_L, to energy stored, W_S, in each hopping transition is represented by $W_L/W_S = (1 - \xi)/\xi$ where ξ is the restraint of screening imposed by the lattice [16]. On the other hand, increase in temperature above 500 °C may increase the number of thermally activated charge carriers (defects) and this will lead to displacement of defects. $Bi_3Zn_{1.84}Nb_3O_{13.84}$ possesses the highest value of the relative permittivity and the lowest value of the dielectric loss in comparison with two analogous systems, $Bi_3Zn_2M_3O_{14}$, (M = Ta and Sb). There is a decrease in the relative permittivity and increase in the dielectric loss passing from the Nb system to the Sb one with the values from ca. 148 to 48 and from ca. 0.002 to 0.006, respectively [22–24]. This could be associated with the substitution of less polarisable Sb^{5+} or Ta^{5+} cations.

4. Conclusion

The cubic pyrochlore, $Bi_3Zn_{1.84}Nb_3O_{13.84}$ exhibits a typical dielectric behaviour in the frequency and temperature ranges studied. High dispersion of permittivity and high dielectric loss at low frequencies and frequency-independent permittivity and dielectric loss at high frequencies (> 100 kHz) with much lower permittivity and dielectric loss are observed. These phenomena could be attributed to the dielectric behaviour of the material, where the conduction mechanism of a hopping type is present. In general, the sample is highly resistive with a high activation energy of ca. 1.59 eV; a high relative permittivity value, 147 and low dielectric loss, 0.002, making it a potential material to be applied in multilayer ceramic capacitors (MLCC).

Acknowledgements

Financial support from the Ministry of Science, Technology and Innovation (MOSTI) is gratefully acknowledged. Special thanks are extended to Prof. A. R. West for his constructive suggestions and comments on impedance study.

References

[1] HEYWANG W., THOMANN H., *Positive Temperature Coefficient Resistors*, [In:] B.C.H Steele (Ed.), *Electronic Ceramics*, Elsevier, London, 1991, p. 29.
[2] RAO C.N.R., GOPALAKRISHNAN J., *New Direction in Solid State Chemistry*, 2nd Ed., Cambridge University Press, Cambridge, 1997.
[3] MUKTHA B., DARRIET J., GIRIDHAR MADRAS., GURU ROW T.N., J. Solid State Chem., 179 (2006), 3919.
[4] SEGAL D.L., *Powders for Electronic*, [In:] B.C.H. Steele (Ed.), *Electronic Ceramics*, Elsevier, London, 1991, p. 185.
[5] CANN D.P., RANDALL C.A., SHROUT T.R., Solid State Commun., 100 (1996), 529.
[6] ZHOU W., J. Solid State Chem., 101 (1992), 1.
[7] SUBRAMANIAM M.A., ARAVAMUDAN G., SUBBA RAO G.V., Progr. Solid State Chem., 15 (1983), 55.
[8] VALANT M., SURUROV J. Am. Ceram. Soc., 88 (2005), 2540.
[9] NINO J.C., LANAGAN M.T., RANDALL C.A., J. Mater. Res., 16 (2001), 1460.
[10] WITHERS R.L., WELBERRY T.R., LARSSON A-K., LIU Y., NOREN L., RUNDLOF H., BRINK F.J., J. Solid State Chem., 177 (2004), 231.
[11] TAN K.B., LEE C.K., ZAINAL Z., MILES G.C., WEST A.R., J. Mater. Chem., 15 (2005), 3501.
[12] VANDERAH T.A., LEVIN I., LUFASO M.W., Eur. J. Inorg. Chem., (2005), 2895.
[13] LEVIN I., AMOS T.G., VANDERAH T.A., RANDALL C.A., LANAGAN M.T., J. Solid State Chem., 168 (2002), 69.
[14] NOBRE M.A.L., LANFREDI S., Mater. Lett., 47 (2001), 362.
[15] NOBRE M.A.L., LANFREDI S., Appl. Phys. Lett., 81 (2002), 451.
[16] HERBERT J.M., *Ceramics Dielectrics and Capacitors*, [In:] D.S. Campbell (Ed.), *The Properties of Dielectrics*, Gordon and Breach Science Publishers, Amsterdam, 1985, p. 9.
[17] DU H.L., YAO X., WANG H., Ferroelectrics, 262 (2001), 89.
[18] RANDALL C.A., NINO J.C., BAKER A., YOUN H-J., HITOMI A., THAYER R., EDGE L.E., SOGABE T., ANDERSON T.D., SHROUT T.R., TROLIER-MCKINSTRY S., LANAGAN M.T., Am. Ceram. Soc. Bull., (2003), 9101.
[19] CLAYTON J., TAKAMURA H., METZ R., TULLER H.L., WUENSCH B.J., J. Electroceramics, 7 (2001), 113.
[20] KAMBA S., POROKHONSKY V., PASHKIN A., BOVTUN V., PETZELT J. Phys. Rev. B., 66 (2002), 054106.
[21] NINO J.C., LANAGAN M.T., RANDALL C.A., J. Applied. Phys., 89 (2001), 4512.
[22] WANG X.L., WANG H., YAO X., J. Am. Ceram. Soc., 80 (1997), 2745.
[23] YOUN H.J., SOGABE T., RANDALL C.A., SHROUT T.P., LANAGAN M.T., J. Am. Ceram. Soc., 84 (2001), 2557.
[24] DU H.L., YAO X., Mater. Electr., 15 (2004), 13.

Received 12 May 2008
Revised 31 October 2008